Stulaigh South, South Uist

Marine Modelling Report

Mowi Scotland Ltd.

December 2022

Mowi Scotland

OFFICE
Mowi, Farms Office, Glen Nevis Business Park
PH33 6RX Fort William

POSTAL
Mowi, Farms Office, Glen Nevis Business Park
PH33 6RX Fort William

PHONE

FAX
-

MAIL
[redacted]

WEB
http://mowiscotland.co.uk

CONTENTS

LIST OF FIGURES

LIST OF TABLES

1. Model Description

1.1 Hydrodynamic Model

The hydrodynamic model used in the Stulaigh South Azamethiphos Dispersion Modelling (Mowi, 2022a) and solids marine modelling (Mowi, 2022b) was FVCOM. FVCOM (Finite Volume Community Ocean Model) is a prognostic, unstructured-grid, finite-volume, free-surface, 3-D primitive equation coastal ocean circulation model developed by the University of Massachusetts School of Marine Science and the Woods Hole Oceanographic Institute (Chen et al., 2003). The model consists of momentum, continuity, temperature, salinity and density equations and is closed physically and mathematically using turbulence closure submodels. The horizontal grid is comprised of unstructured triangular cells and the irregular bottom is presented using generalized terrain-following coordinates. The General Ocean Turbulent Model (GOTM) developed by Burchard's research group in Germany (Burchard, 2022) has been added to FVCOM to provide optional vertical turbulent closure schemes. FVCOM is solved numerically by a second-order accurate discrete flux calculation in the integral form of the governing equations over an unstructured triangular grid. This approach combines the best features of finite-element methods (grid flexibility) and finite-difference methods (numerical efficiency and code simplicity) and provides a much better numerical representation of both local and global momentum, mass, salt, heat and tracer conservation. The ability of FVCOM to accurately solve scalar conservation equations in addition to the topological flexibility provided by unstructured meshes and the simplicity of the coding structure has made FVCOM ideally suited for many coastal and interdisciplinary scientific applications.

The mathematical equations are discretized on an unstructured grid of triangular elements which permits greater resolution of complex coastlines, such as typically found in Scotland. Therefore greater spatial resolution in near-shore areas can be achieved without excessive computational demand.

1.2 Particulate Deposition Model

The regional particulate deposition modelling, performed using the UnPTRACK model (Gillibrand 2021), simulated the settling of waste solids (waste feed and faeces) discharged from pens during a production cycle. Deposition from pens at the proposed site of Stulaigh South and the neighbouring site at Stulaigh were simulated. Particles were discharged continuously from each pen, with each numerical particle representing 2.5 kg of particulate waste. Feed and faecal particles were assigned settling velocities within the range of 0.095 m s^{-1} ±10% and 0.032 m s^{-1} ± 10% respectively, the same as the values used by NewDepomod.

The particle tracking model used a hydrodynamic model simulation from June – October 2020 (see §5) to calibrate the particle tracking model against benthic survey data collected at the Stulaigh site on 6th October 2020. The calibrated model was then used to predict regional deposition from both Stulaigh and Stulaigh South sites (Mowi, 2022b).

When a particle reaches the seabed due to its settling velocities, it may be resuspended into the water column and be subject again to advection and diffusion. Resuspension is modelled using a stochastic approach, whereby a probability of resuspension is specified for each settled

particle every time step. In the present simulations, the probability of resuspension, P, was calculated by:

$$P = c_r(\tau_b - \tau_{bc})e^{-t_p/\lambda}$$

where $\tau_b = \rho u_*^2$ is the bed shear stress derived from the local modelled current speed, τ_{bc} is the minimum critical shear stress required to erode particles off the seabed, c_r is a resuspension constant, t_p is the age of the particle since settlement on the seabed and λ is a timescale for consolidation. With this approach, the probability of particle erosion increases with the excess shear stress, but decreases as the time since settlement increases. This reflects a likelihood that as particles remain on the seabed they become consolidated into the sediment layer and therefore less likely to be resuspended. The parameters c_r, τ_{bc} and λ are tunable coefficients that can be used to calibrate the deposition model. Numerous model simulations were performed with varying values of c_r, τ_{bc} and λ to find the combination producing the best agreement between modelled deposition and benthic health data from a seabed monitoring survey during October 2020. For the simulations presented in §6, values of c_r = 0.2, τ_{bc} = 0.02 Pa and λ = 4 days were used. A bed roughness scale of z_0 = 0.01 m was used to calculate the bed shear stress from the local current speed.

2. Configuration and Boundary Forcing for Stulaigh South

The unstructured mesh to be used in the marine modelling is shown in Figure 1. The model resolution was enhanced in the area around the Mowi site at Stulaigh South (Figure 2). The spatial resolution of the model varied from 25m in some inshore waters and round the farm pens to 500 m along the open boundary. The model consisted of 7,310 nodes and 13,699 triangular elements.

Model bathymetry was taken from the European Marine Observation and Data Network (EMODnet, https://www.emodnet-bathymetry.eu/), supplemented by a multibeam survey undertaken in June 2021 (Figure 3).

The model was forced along its open boundary time series of sea surface height (SSH) at each boundary node for the relevant simulation periods; FVCOM appears to perform better with time series boundary forcing than when tidal constituents are used. The SSH time series were generated using RiCOM hydrodynamic model (Walters et al., 2010; Gillibrand et al., 2016) on the ECLH grid, which was, in turn, forced by eight tidal constituents (M_2, S_2, N_2, K_2, O_1, K_1, P_1 and Q_1) taken from the full Marine Scotland Scottish Shelf Model (SSM; Wolf et al., 2016). Wind speed and direction data were taken from the European Centre for Medium-Range Weather Forecasts (ECMWF) ERA5 reanalysis product (https://www.ecmwf.int/en/forecasts/datasets/reanalysis-datasets/era5), with data interpolated onto the nodal locations of the model mesh.

The model was run in 3D mode with 10 equally spaced layers in the vertical. Freshwater discharges were input to the model domain at four locations (Figure 1). The freshwater flux data at each location was based on river flow data for stations Abhainn Roag at Mill Croft from the Centre for Ecology and Hydrology (CEH) National River Flux Archive (NRFA), weighted by catchment area for Loch Boisdale and Loch Eynort. Catchment areas for the two central streams discharging north and south of Stulaigh Island were estimated from maps.

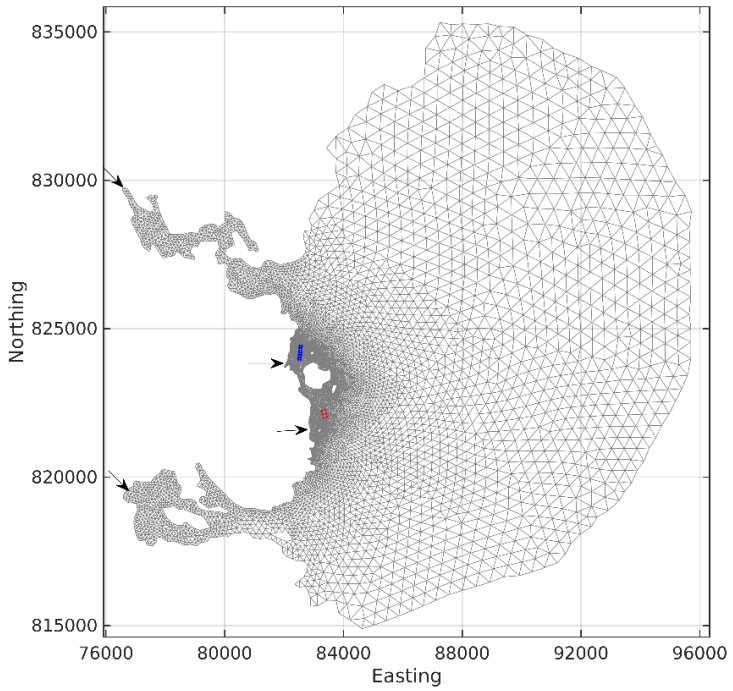

Figure 1. The full mesh and domain of the modelling study, with the proposed cage locations indicated (o) and the pens at the neighbouring Stulaigh site also marked (o). Locations of ADCP deployments (▲) and freshwater inputs to the model (→) are marked.

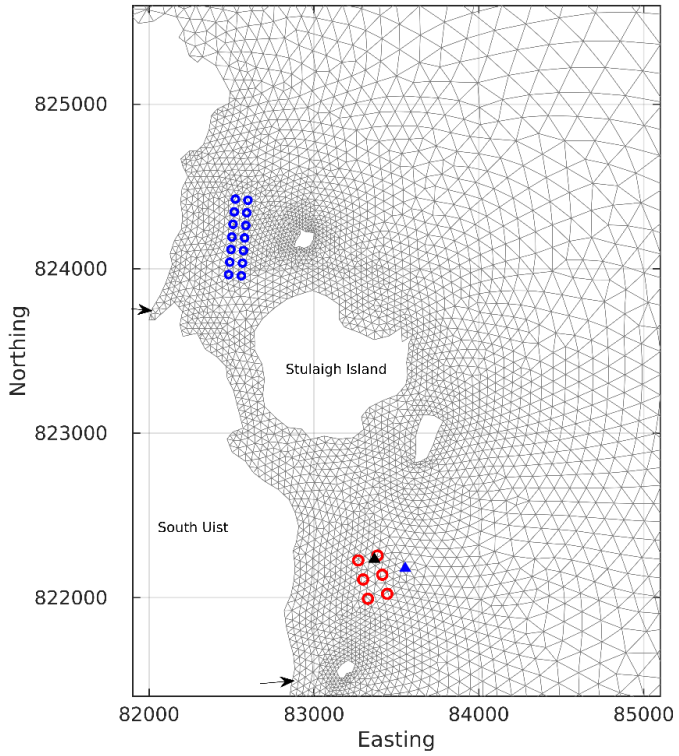

Figure 2. The unstructured mesh around the Stulaigh South site in the modified model grid, with the proposed cage locations indicated (o) and the pens at the neighbouring Stulaigh site also marked (o). Locations of ADCP deployments (▲) and freshwater inputs to the model (→) are marked.

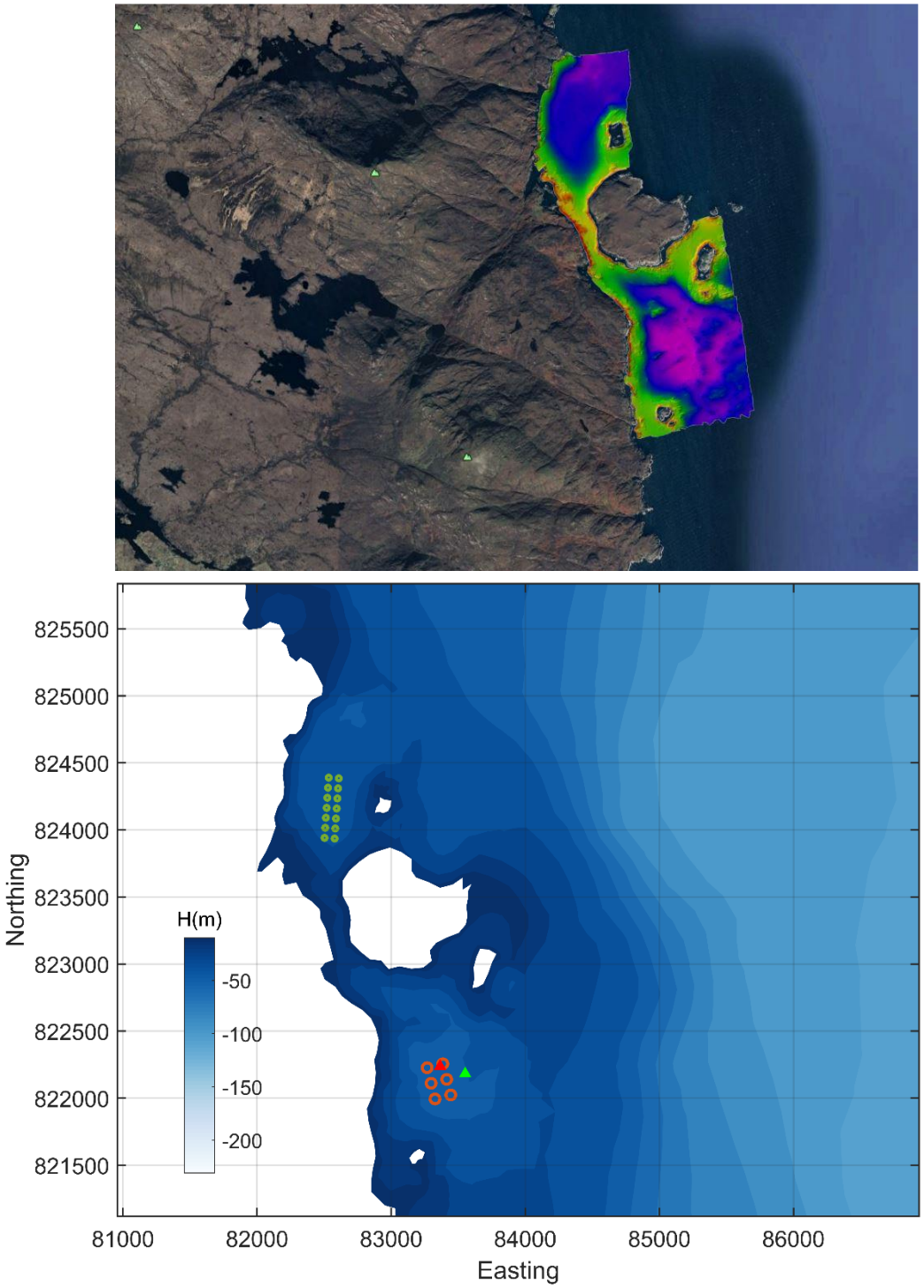

Figure 3. Multibeam survey of bathymetry around Stulaigh Island (top) from June 2021. Model water depths (m) in the area around the proposed salmon farm (bottom), incorporating the multibeam data. The proposed cage locations indicated (○). The existing pens at Stulaigh (○) and the ADCP deployment locations ID208 (▲) and ID224 (▲) are indicated.

3. Model Calibration and Validation

For the current study, the model was further calibrated against hydrographic data collected in the region of the farm site in 2018 (Figure 4). The data are described in the relevant hydrographic reports. In March 2018, an Acoustic Doppler Current Profiler (ADCP) was deployed close to the proposed location of the Stulaigh South site until May 2018 ID208). A second ADCP was deployed close to the proposed location of the Stulaigh South site from May 2018 until August 2018 (ID224). In all, 123 days of current data were used in this application. The ADCP deployments provided both current velocity and seabed pressure data, which were used to calibrate and validate the modelled velocity and sea surface height.

For each simulation, the model was "spun-up" for three days with boundary forcing ramped up from zero over a period of 48 hours. The model state at the end of the 72-hour spin-up period was stored, and the main simulations "hot-started" from this state.

The following main simulations were performed, corresponding with the dates of the ADCP deployments:

(i) Calibration: 8th March 2018 – 23rd May 2018 (ID208)
(ii) Validation: 22nd May 2018 – 14th August 2018 (ID224)

[Note that the dates above refer to the main simulations and that the spin-up simulations ran for three days prior to the start dates given above.]

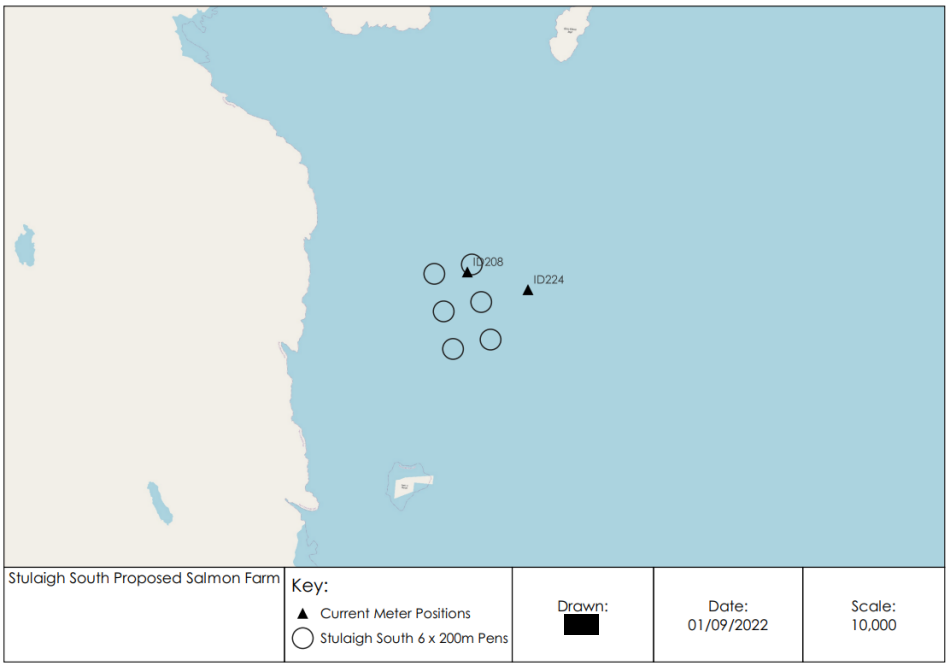

Figure 4. Locations of the ADCP deployments relative to the proposed pens for Stulaigh South farm.

Model performance is assessed using three metrics: the mean absolute error (MAE), the root-mean-square error (RMSE) and the model skill (d_2). The first two are standard measures of model accuracy; the third, d_2, is taken from Willmott et al. (1985) and lies in the range $0 \leq d_2 \leq 1$, with $d_2 = 0$ implying zero model skill and $d_2 = 1$ indicating perfect skill.

3.1 Calibration: March - May 2018, ID208

The calibration used observed depth and current velocity from the ADCP location to compare with modelled sea surface height (SSH) and velocity (ADCP deployment ID208). The model was calibrated by varying the value of the bottom roughness lengthscale, z_0, which determines the frictional effect of the seabed on the flow. Simulations were performed with a range of values of z_0 varying over the range $0.001 \leq z_0 \leq 0.01$. The influence of the Smagorinsky coefficient for horizontal viscosity and diffusivity was also explored. After a number of simulations, a final parameter set was selected (Table 1).

Table 1. Parameter values chosen for the FVCOM model during the calibration simulations.

Parameter Description	Value
Bottom roughness lengthscale, z_0	0.001
Smagorinsky coefficient for horizontal diffusion	0.1
Number of vertical layers	10
Barotropic model time step (s)	0.5
Baroclinic model time step (s)	5.0

The results of the calibration exercise are presented in Figure 5 – Figure 8 and Table 2. *Model performance for SSH at the ADCP location from March – May 2018 (ID208).*

	SSH
Model skill, d^2	0.99
Mean Absolute Error (MAE) (m/s)	0.15
Root-Mean-Square Error (RMSE) (m/s)	0.18

and Table 2. At the ADCP location, the sea surface height was reasonably accurately modelled, with model skill of 0.99. The mean absolute error (MAE) and root-mean-square error (RMSE) values of 0.15 m and 0.18m (Table 2. *Model performance for SSH at the ADCP location from March – May 2018 (ID208).*

	SSH
Model skill, d^2	0.99
Mean Absolute Error (MAE) (m/s)	0.15
Root-Mean-Square Error (RMSE) (m/s)	0.18

) are about 3.3% and 3.9% of the spring tide range (4.59m) respectively.

For the calibration period, the model skill scores, RMSE and MAE for the East and North components of velocity are shown in Table 3 and Figure 6. The scatter plots and histograms demonstrate that the modelled current had broadly the same magnitude and direction characteristics as the observed data (Figure 7 and Figure 8).

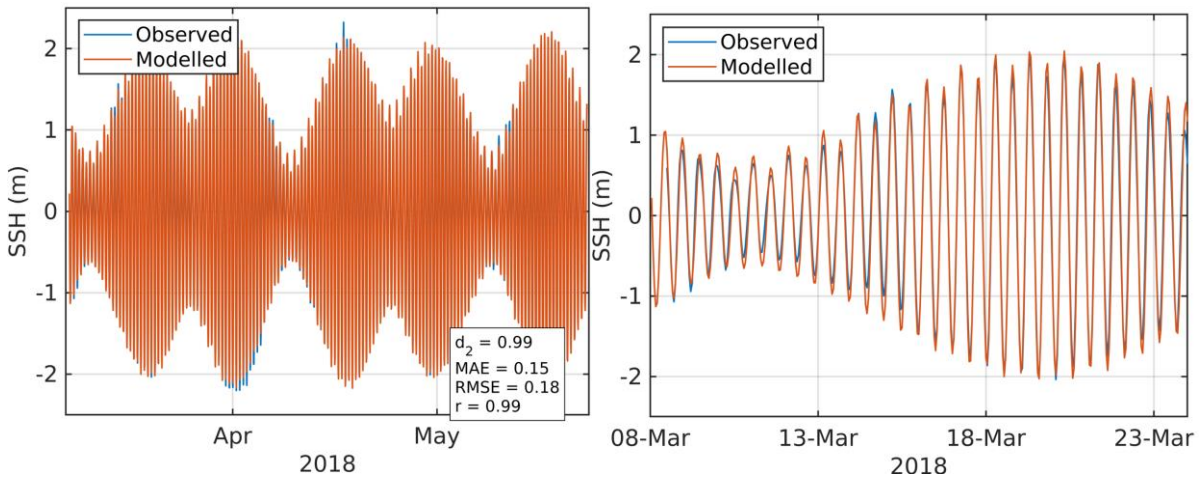

Figure 5. Comparison between observed and modelled sea surface height from March – May 2018 (ADCP deployment ID208) using model parameter values from Table 1. Both the full record (left) and a subset of 15 days (right) are shown. Observed data are in blue, model results in red.

Table 2. Model performance for SSH at the ADCP location from March – May 2018 (ID208).

	SSH
Model skill, d^2	0.99
Mean Absolute Error (MAE) (m/s)	0.15
Root-Mean-Square Error (RMSE) (m/s)	0.18

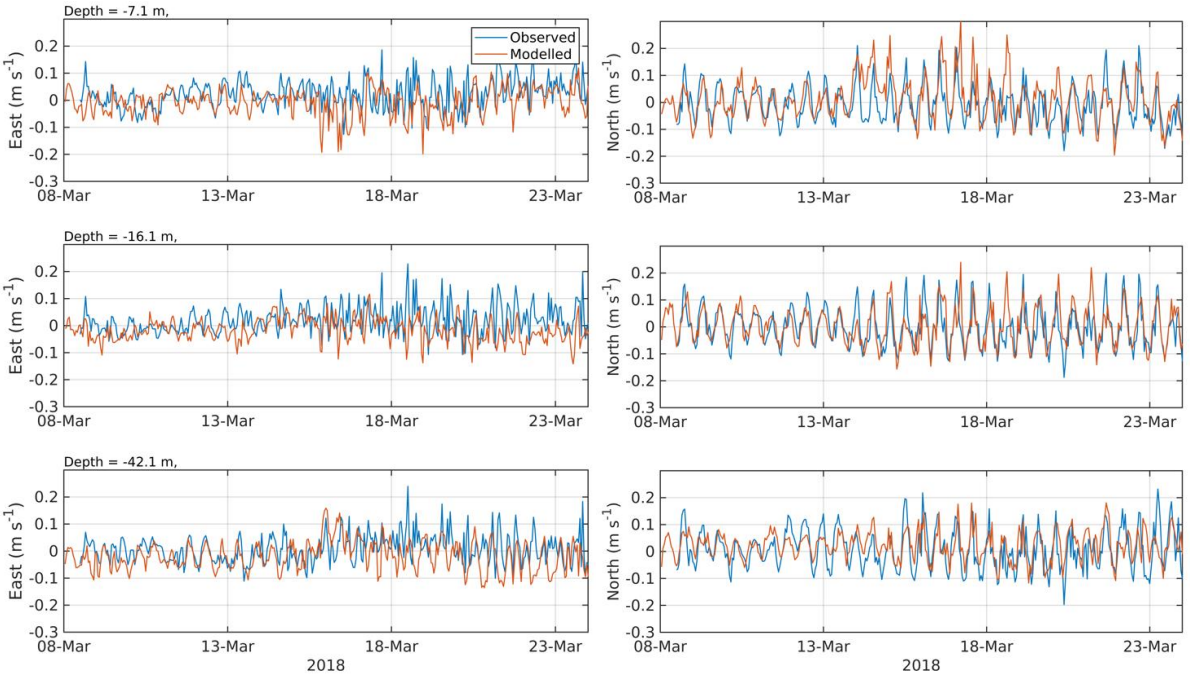

Figure 6. Comparison between observed and modelled East (left) and North (right) components of velocity at the ADCP location for 15 days in March 2018 (ID208) for the three depths, sub-surface (top), cage bottom (middle), near bed (bottom). Observed data are in blue, model results in red.

Table 3. Model performance statistics for East and North velocity at the ADCP location from March – May 2018 (ID208) for the three depths.

		East	North
Sub-surface cell	Model skill, d^2	0.36	0.54
	Mean Absolute Error (MAE) (m/s)	0.07	0.08
	Root-Mean-Square Error (RMSE) (m/s)	0.09	0.11
Mid-depth cell	Model skill, d^2	0.45	0.78
	Mean Absolute Error (MAE) (m/s)	0.06	0.05
	Root-Mean-Square Error (RMSE) (m/s)	0.08	0.06
Near-bed cell	Model skill, d^2	0.43	0.60
	Mean Absolute Error (MAE) (m/s)	0.06	0.06
	Root-Mean-Square Error (RMSE) (m/s)	0.08	0.07

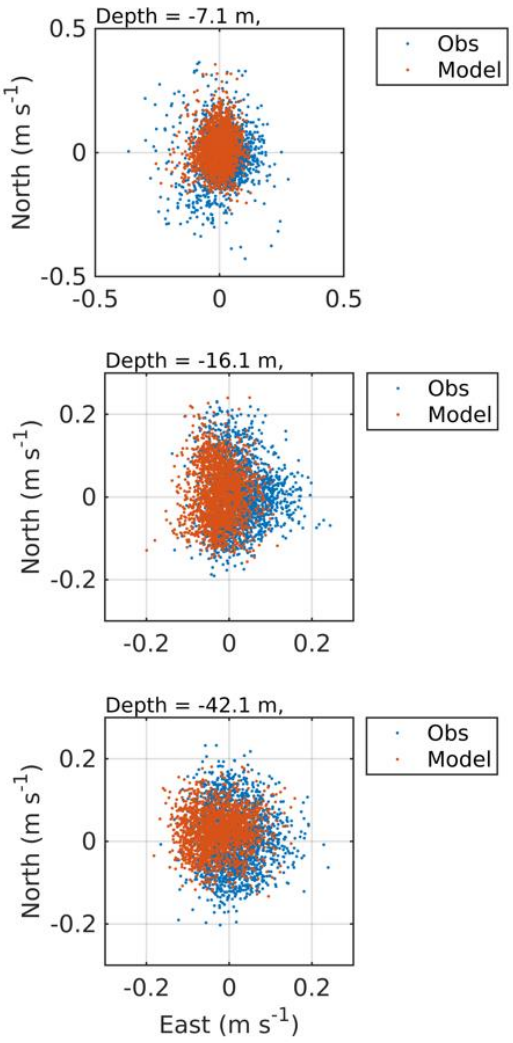

Figure 7. Scatter plots of observed and modelled velocity at the ADCP location from March – May 2018 (ID208) for the three depths, sub-surface (top), cage bottom (middle), near bed (bottom). Observed data are in blue, model results in red.

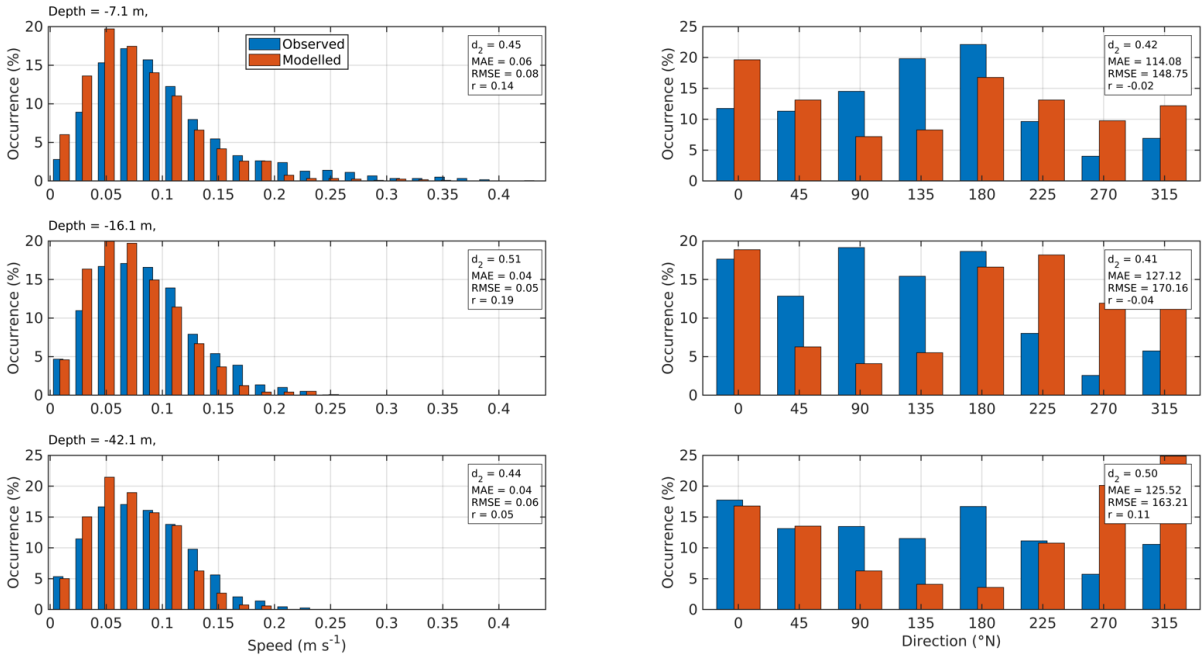

Figure 8. Histograms of observed and modelled speed (left) and direction (right) at the ADCP location from March – May 2018 (ID208) for the three depths, sub-surface (top), cage bottom (middle), near bed (bottom). Observed data are in blue, model results in red.

3.2 Validation: May – August 2018, ID224

At the ADCP location, the sea surface height was reasonably accurately modelled, with model skill of 0.97 (Figure 9, Table 4). The mean absolute error (MAE) and root-mean-square error (RMSE) values of 0.28 m and 0.34 m are about 6.1% and 7.4% of the spring tide range (4.6m) respectively.

For the calibration period, the skill scores, RMSE and MAE for the modelled East and North components of velocity (Figure 10) are shown in Table 5. The scatter plots and histograms demonstrate that the modelled current had broadly the same magnitude and direction characteristics as the observed data (Figure 11 and Figure 12).

Table 4. Model performance for SSH at the ADCP location from May – August 2018 (ID224).

	SSH
Model skill, d^2	0.97
Mean Absolute Error (MAE) (m/s)	0.28
Root-Mean-Square Error (RMSE) (m/s)	0.34

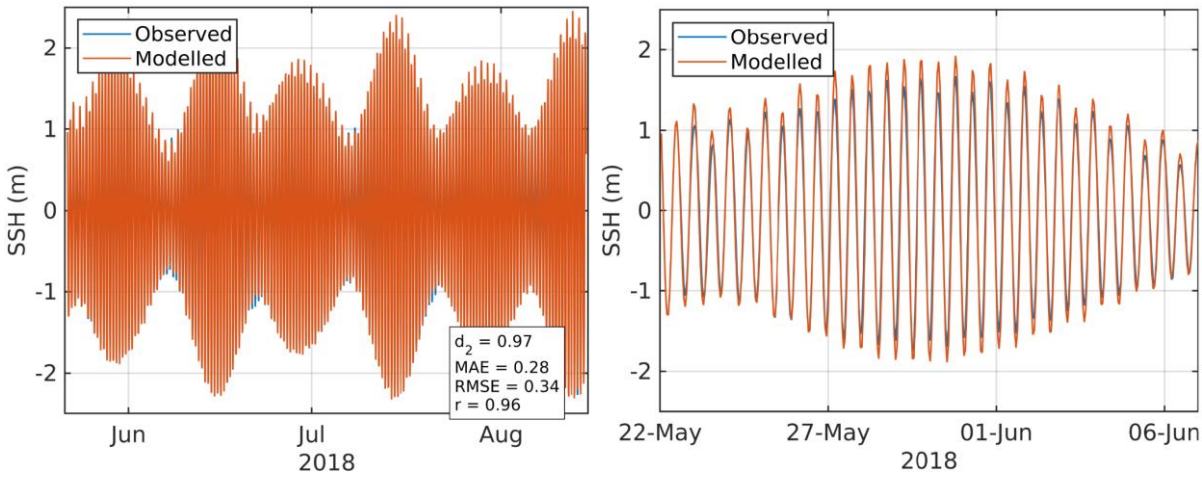

Figure 9. Comparison between observed and modelled sea surface height from May – August 2018 (ADCP deployment ID224) using model parameter values from Table 1. Both the full record (left) and a subset of 15 days (right) are shown. Observed data are in blue, model results in red.

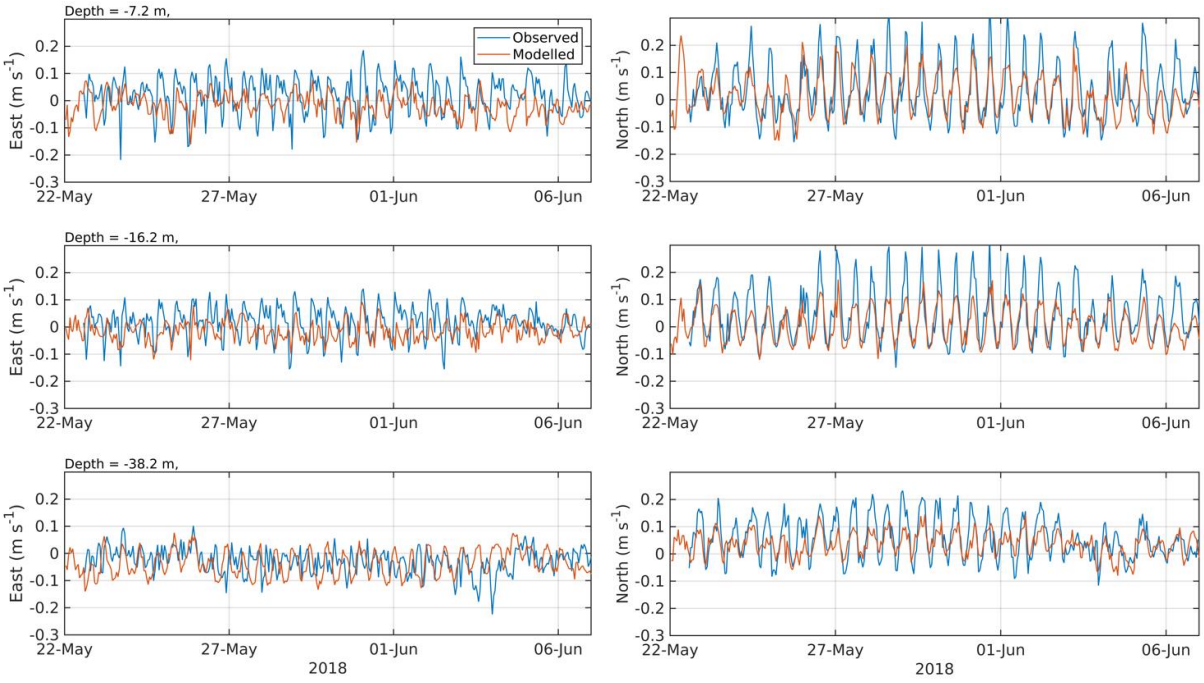

Figure 10. Comparison between observed and modelled East (left) and North (right) components of velocity at the ADCP location for 15 days in May - June 2018 (ID224) for the three depths – surface (top), mid-depth (middle), near-bed (bottom). Observed data are in blue, model results in red.

Table 5. Model performance statistics for East and North velocity at the ADCP location from May – August 2018 (ID224) for the three depths.

		East	North
Sub-surface cell	Model skill, d^2	0.50	0.79
	Mean Absolute Error (MAE) (m/s)	0.06	0.07
	Root-Mean-Square Error (RMSE) (m/s)	0.08	0.09
Mid-depth cell	Model skill, d^2	0.52	0.82
	Mean Absolute Error (MAE) (m/s)	0.05	0.06
	Root-Mean-Square Error (RMSE) (m/s)	0.07	0.08
Near-bed cell	Model skill, d^2	0.45	0.64
	Mean Absolute Error (MAE) (m/s)	0.06	0.06
	Root-Mean-Square Error (RMSE) (m/s)	0.07	0.07

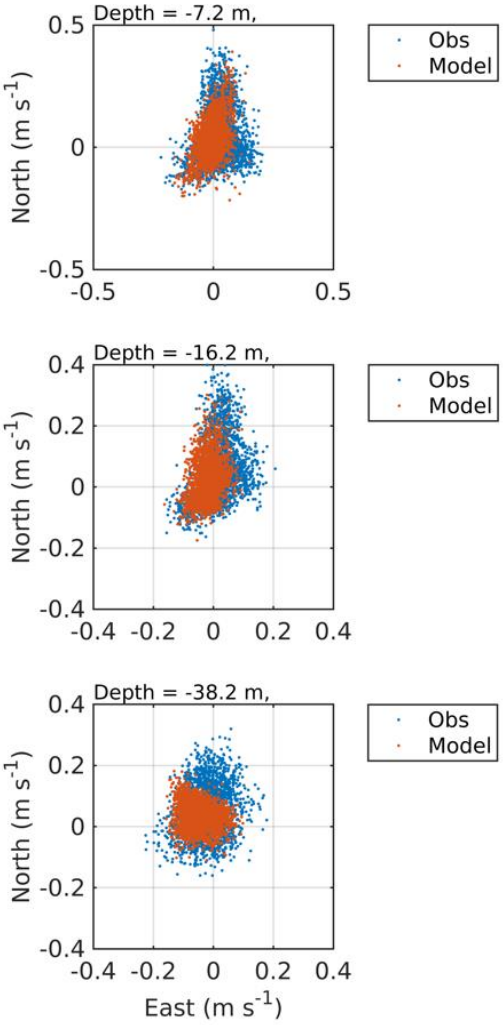

Figure 11. Scatter plot of observed and modelled velocity at the ADCP location from May – August 2018 (ID224) for the three depths, surface (top), mid-depth (middle), near-bed (bottom). Observed data are in blue, model results in red.

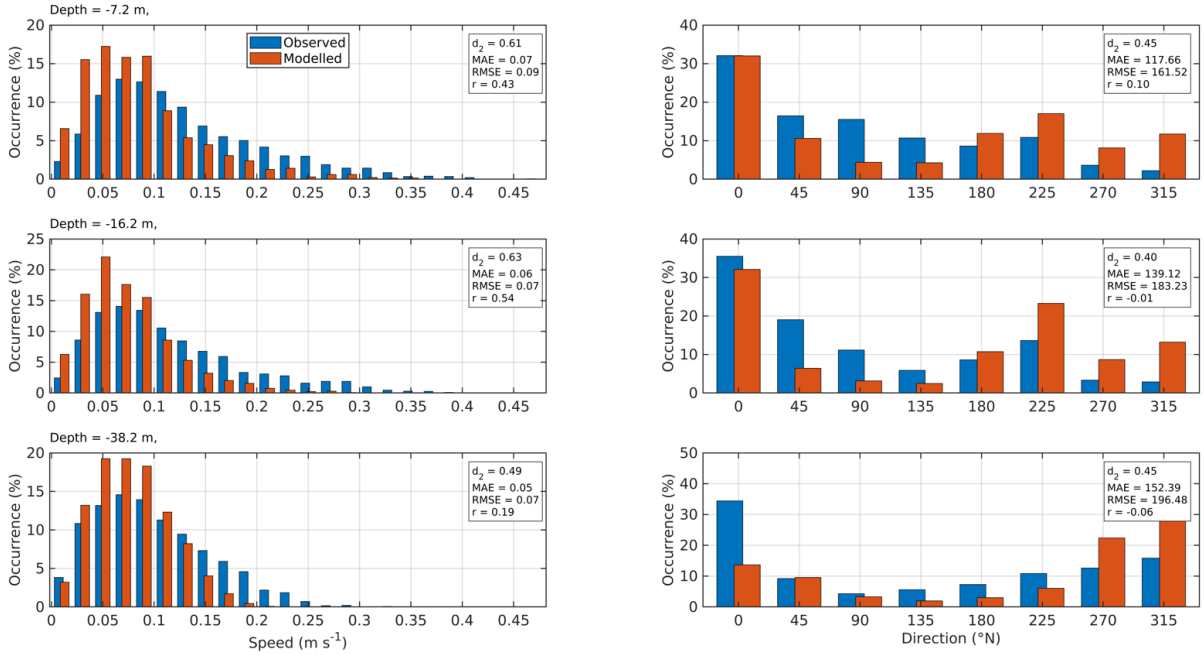

Figure 12. Histograms of observed and modelled current speed (left) and direction (right) at the ADCP location from May – August 2018 (ID224) for the three depths, surface (top), mid-depth (middle), near-bed (bottom). Observed data are in blue, model results in red.

4. Modelled Flow Fields (ID208)

Modelled flood and ebb velocity vectors at spring tides are illustrated in Figure 13. The Stulaigh South site is exposed to the strong currents from the Sea of the Hebrides, particularly form the south. The prevailing flow at the site was northwards, whereas the prevailing flow along the east coast of South Uist is expected to be southward as the Scottish Coastal Current bifurcates in the Little Minch (Hill et al., 1997). Northward currents during flood tide are strong from the south around the Stulaigh South site (Figure 13), but flow patterns from the north during ebb tides are complicated by the presence of Stulaigh Island and the satellite islands to the southwest of it (Figure 13), perhaps partly explaining the northward tendency at the site.

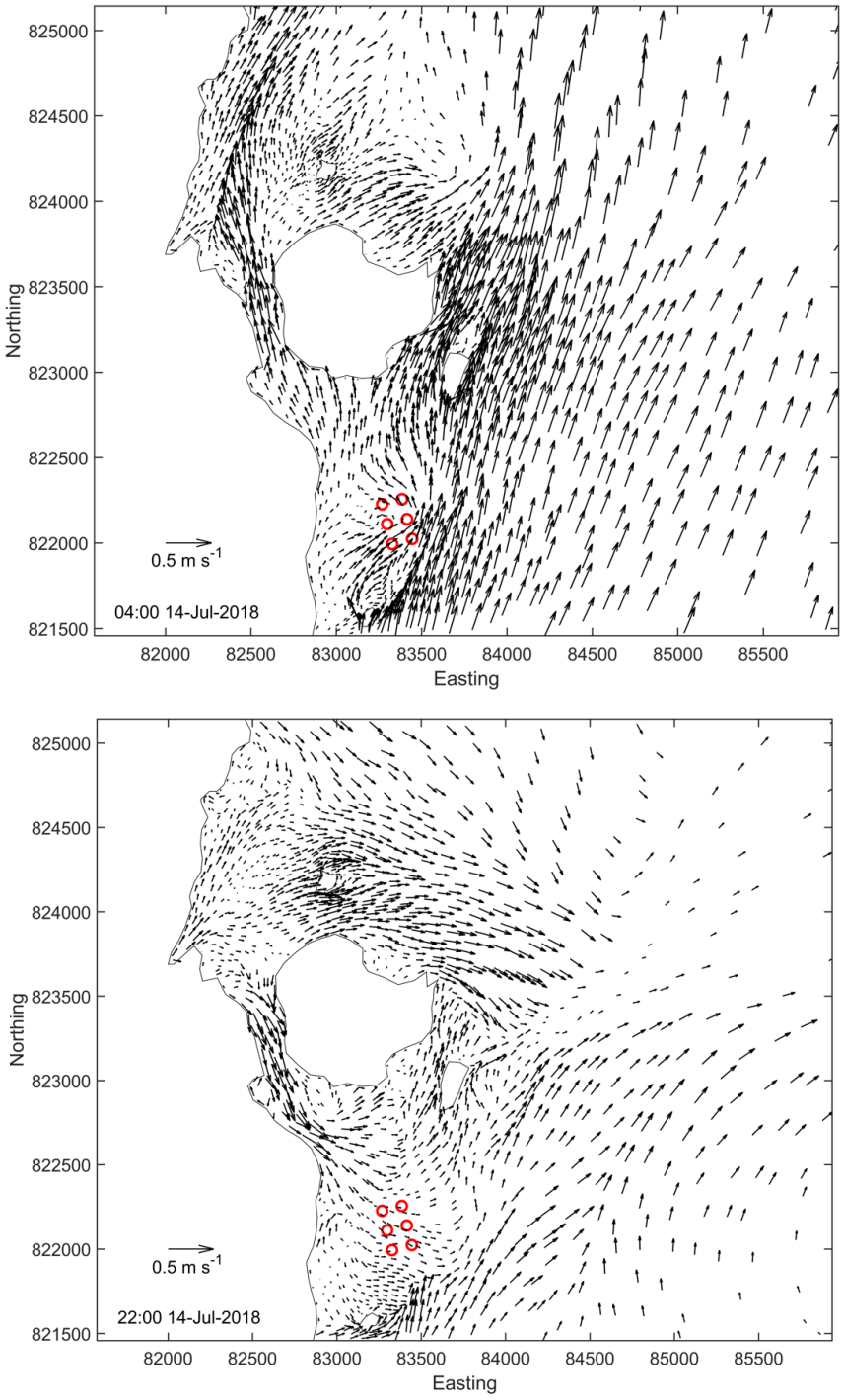

Figure 13. Modelled flood (top) and ebb (bottom) surface current vectors during spring tides on 14th July 2018. For clarity, only 25% of the model current vectors are shown.

5. Simulation for Regional Solids Waste Modelling

In order to calibrate the regional particle tracking model against seabed survey data collected at Stulaigh, a hydrodynamic simulation was performed for the period leading up to the date of the seabed survey, 23rd June – 6th October 2020. The Stulaigh seabed survey was carried out on 6th October 2020.

Modelled velocity time series for the locations where ADCP deployments ID208 and ID224 were made are shown in Figure 14 and Figure 15 respectively. Scatter plots of the velocity data from both locations are shown in Figure 16. Data were not collected for this period, so just the modelled velocities are shown. The magnitude and direction of the modelled currents can be compared with the data collected by ID208 and ID224 and shown in §3.1 and §3.2 above.

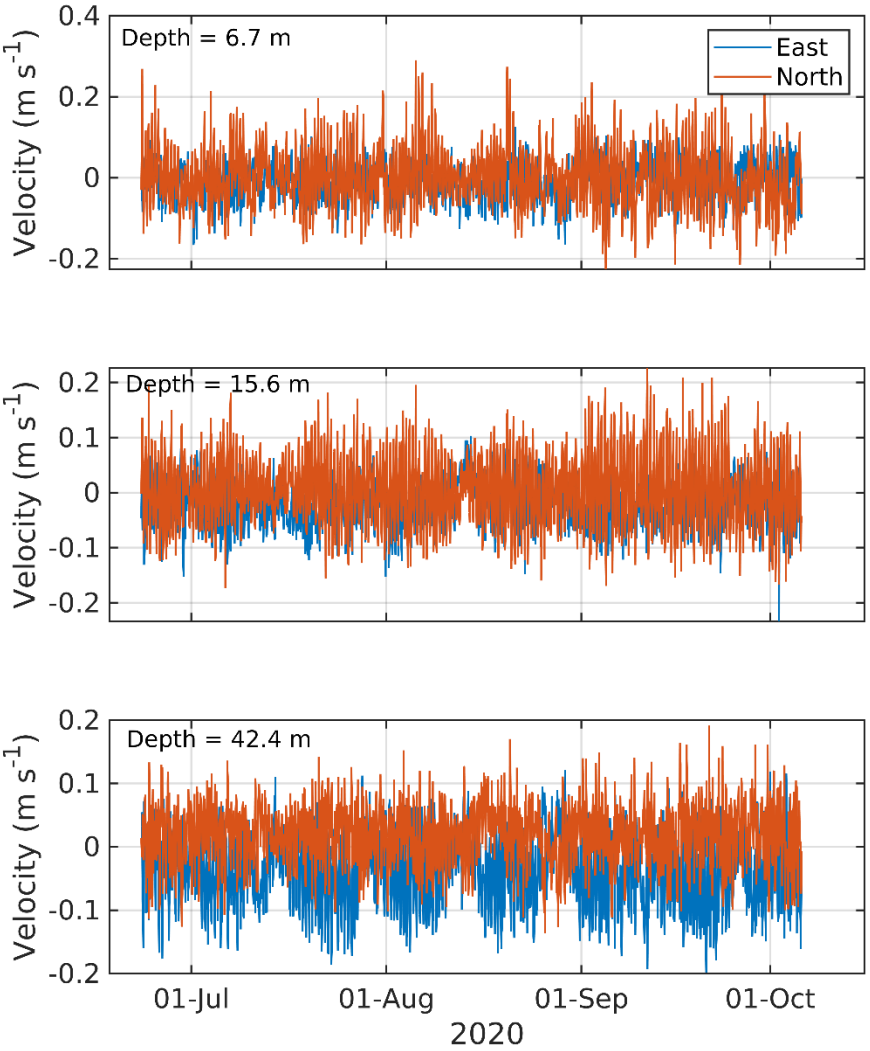

Figure 14. Modelled time series of east and north velocity at three depths, 6.7 m (top), 15.6m (middle) and 42.4m (bottom) at the location of ID208 but during June – October 2020.

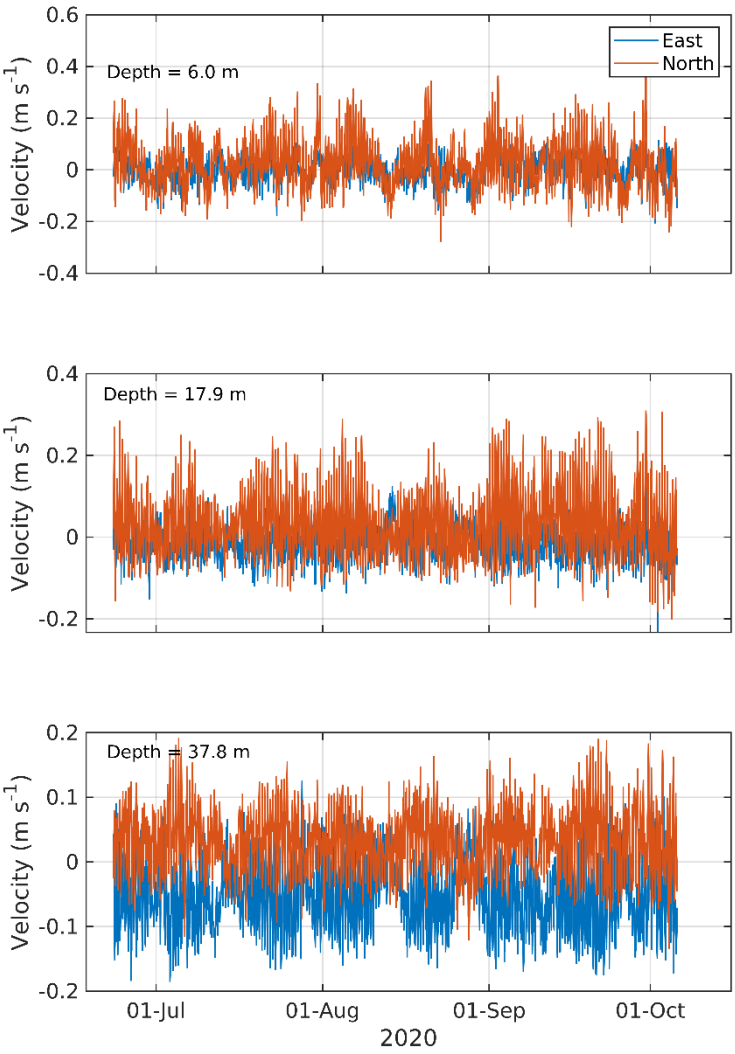

Figure 15. Modelled time series of east and north velocity at three depths, 6.0 m (top), 17.9m (middle) and 37.8 m (bottom) at the location of ID224 but during June – October 2020.

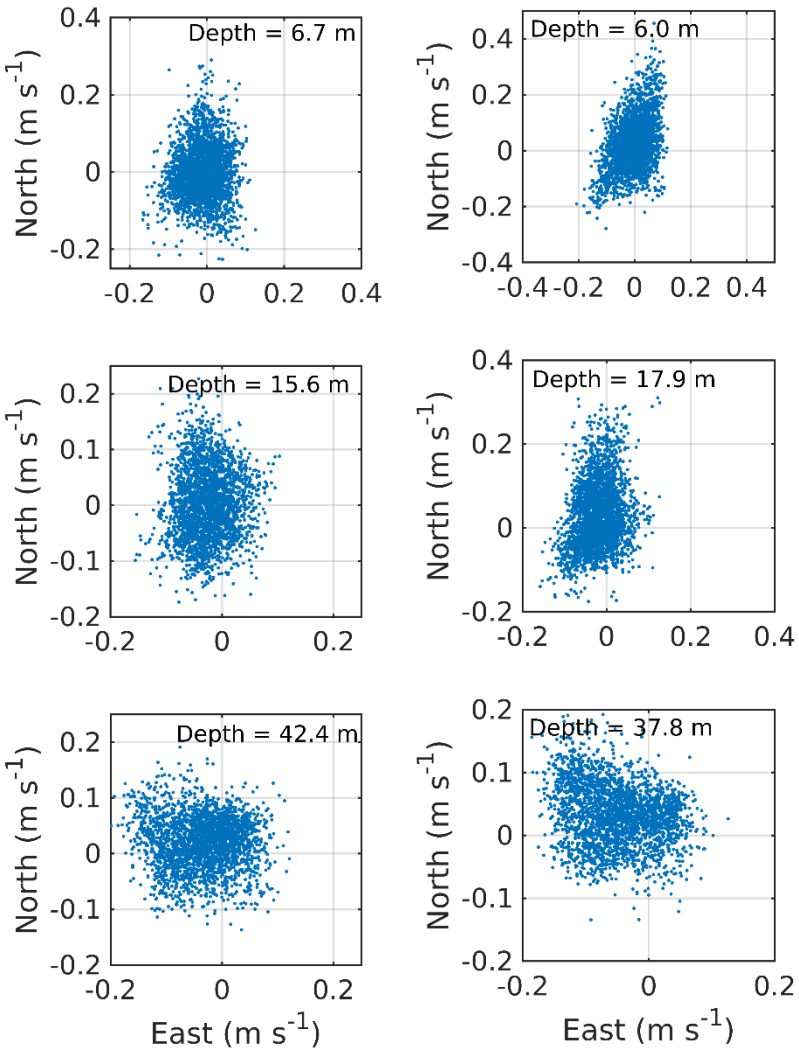

Figure 16. Scatter plots of east and north velocity at three depths at the locations of ID208 (left) and ID224 (right) during June – October 2020.

6. Regional Solids Waste Model Calibration

The particle tracking model was calibrated against seabed survey data collected in October 2020 from the nearby Stulaigh site (Figure 2). Pen locations for Stulaigh used in the modelling are given in Table 6. Daily recorded feed inputs were used to estimate wasted feed and faecal waste quantities, using the standard formulae (SEPA, 2019), at Stulaigh (Figure 17). The model was run for the production cycle from 13th August 2019 – 6th October 2020, using the flow fields from 23rd June – 6th October 2020 described in §5.

Model predictions of deposition over the final 90 days of the simulation (8th July – 6th October 2020) were averaged to give the mean deposition (Figure 18). Comparison between modelled deposition and observed Infaunal Quality Index (IQI) resulted in a root-mean-square error (RMSE) of 0.075 (Figure 19), calculated using the logistic function shown in Figure 19 to convert modelled deposition to predicted IQI.

Table 6. Details of the 14 x 120m pen centre locations and net depths used in the modelling for the neighbouring site at Stulaigh.

Pen	Easting	Northing	Net Depth (m)
1	82599	824416	16
2	82523	824423	16
3	82592	824340	16
4	82516	824346	16
5	82586	824263	16
6	82509	824270	16
7	82579	824187	16
8	82502	824193	16
9	82572	824110	16
10	82496	824117	16
11	82566	824034	16
12	82489	824040	16
13	82559	823957	16
14	82482	823964	16

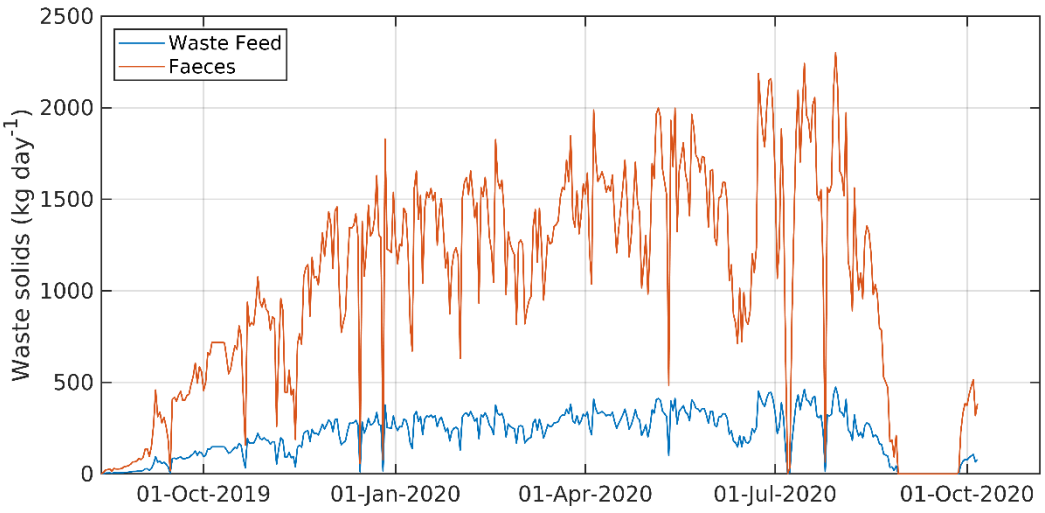

Figure 17. Time series of waste solids discharged from Stulaigh salmon farm from 13th August 2019 – 6th October 2020. The daily quantities of waste feed and faeces were used by the UnPTRACK model to simulate deposition leading up to the seabed survey on 6th October 2020.

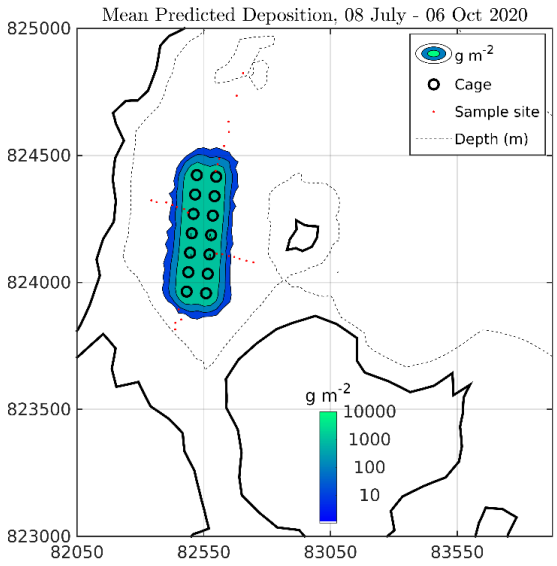

Figure 18. Predicted mean deposition (g m^{-2}) over the final 90 days (8th July – 6th October 2020) of the simulation of deposition from the Stulaigh site using recorded feed to estimate daily waste inputs to the model. Pen locations (O) and sample locations (●) from the October 2020 seabed survey are indicated.

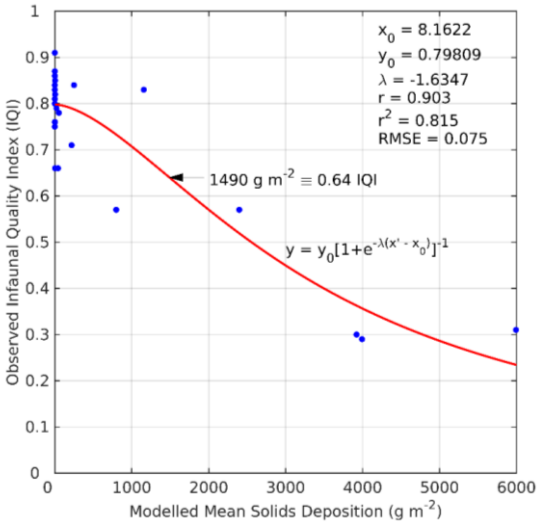

Figure 19. Modelled mean deposition (●) at 26 sample locations from the October 2020 seabed survey plotted against the observed Infaunal Quality Index (IQI) at the sample locations. A logistic function was fitted to the data (—) giving a critical deposition threshold of 1490 g m^{-2}.

The configuration of the model obtained from this calibration process was used to predict solids deposition arising from the proposed farm at Stulaigh South (Mowi, 2022b) i.e. the predicted benthic IQI, ŷ, will be calculated from the logged modelled deposition, x', using the equation

$$\hat{y} = \frac{0.798}{[1 + e^{1.6347(x' - 8.1622)}]}$$

7. References and Bibliography

Burchard, H., 2002. Applied turbulence modelling in marine waters. Spring:Berlin-Heidelberg-New York-Barcelona-Hong Kong-London-Milan-Paris-Tokyo, 215pp.

Chen, C., H. Liu, and R.C. Beardsley, 2003. An unstructured, finite-volume, three-dimensional, primitive equation ocean model: Application to coastal ocean and estuaries. J. Atmos. Ocean. Tech., 20, 159 – 186.

Gillibrand, P.A., 2021. Unptrack User Guide. Mowi Scotland Ltd., February 2021, 31pp. https://github.com/gillibrandpa/unptrack

Gillibrand, P.A., Walters, R.A., and McIlvenny, J., 2016. Numerical simulations of the effects of a tidal turbine array on near-bed velocity and local bed shear stress. *Energies*, vol 9, no. 10, pp. 852. DOI: 10.3390/en9100852

Hill A.E., K.J. Horsburgh, R.W. Garvine, P.A. Gillibrand, G. Slesser, W.R. Turrell and R.D. Adams, 1997. Observations of a density-driven recirculation of the Scottish coastal current in the Minch. Estuarine Coastal and Shelf Science, 45, 473-484.

Mowi, 2022a. Stulaigh South Azamethiphos Dispersion Modelling Report. Mowi Scotland Ltd., September 2022, 28 pp.

Mowi, 2022b. Stulaigh South Waste Solids & In-feed Medicine Deposition Modelling Report. Mowi Scotland Ltd., December 2022, 14 pp.

Walters, R.A.; Gillibrand, P.A.; Bell, R.; Lane, E.M. 2010. A Study of Tides and Currents in Cook Strait, New Zealand. Ocean Dyn., 60, 1559-1580.

Wolf, J., Yates, N., Brereton, A., Buckland, H., De Dominicis, M., Gallego, A., Murray, R O'Hara, 2016. The Scottish Shelf Model:Part 1: Shelf-Wide Domain. Scottish Marine and Freshwater Science Vol 7 No 3, 153 pp.